CHEMISTRY

Origin of sulfur allotropes on the carbonaceous asteroid Ryugu and implications to the sulfur chemistry in the interstellar medium

Mason McAnally[1,2], Chaojiang Zhang[1,2], Jia Wang[1,2], Ashanie Herath[1,2], Andrew M. Turner[1,2], Ralf I. Kaiser[1,2]*

The unexpected detection of the sulfur allotropes (S_8, S_7, and S_6) on the carbonaceous asteroid Ryugu following the Hayabusa2 mission has offered insights into the unconventional sulfur chemistry in space. These molecules can be traced to processes occurring in the early stages of the evolution of cold molecular clouds, where interstellar icy mantles facilitate the formation of complex sulfur-bearing species by energetic processing. Exploiting interstellar ice analogs, the present study affords compelling evidence on the production of sulfur allotropes (S_8, S_7, and S_6) in sulfur-doped interstellar analog ices composed of sulfur dioxide (SO_2), hydrogen sulfide (H_2S), and water (H_2O) using soft photoionization reflectron time-of-flight mass spectrometry. The synthesis of these allotropes offers fundamental insights into their possible origin on Ryugu while also presenting a plausible mechanism for the sulfur depletion in cold molecular clouds. Notably, the oxidation of sulfur (-II) in hydrogen sulfide (H_2S) represents the driving force in sulfur allotrope formation.

INTRODUCTION

Sophisticated analyses of returned samples from the carbonaceous asteroid Ryugu within the framework of the Hayabusa2 mission revealed an astonishing array of sulfur-bearing species ranging from alkylsulfonic acids (R-SO_3H with R being an alkyl group), polythionic acids (SO_3-S_n-SO_3; $n = 1$ to 6) to sulfur allotropes (S_n; $n = 6$ to 8) (*1*). The detection of sulfur allotropes with octasulfur (S_8) accompanied by a few percent of heptasulfur (S_7) and hexasulfur (S_6) represents the first detection of large sulfur material in asteroids providing valuable chemical insight into formation products directly from astrophysical environments (*1*). Nguyen *et al.* (*2*) proposed a critical link between refractory material—such as the sulfur allotrope octasulfur (S_8)—on the carbonaceous asteroid Ryugu and ices on dust grains which may facilitate the production of sulfur allotropes through exposure by galactic cosmic rays (GCRs) (Fig. 1) (*3*–*5*).

However, the current understanding of the sulfur chemistry in ices of molecular clouds has just scratched the surface (*6*–*8*). The unraveling of the formation of sulfur allotropes (S_8, S_7, and S_6) on the carbonaceous asteroid Ryugu has been elusive to date and hence requires laboratory experiments linking the unconventional nonequilibrium chemistry in low temperature ices to the origin of these sulfur allotropes. The presence of these refractory allotropes on Ryugu may also offer key insight into the long-standing puzzle of sulfur depletion in dense molecular clouds, where observed gas-phase sulfur is underabundant by two to three orders of magnitude compared to cosmic ratios (*9*–*13*). The diffuse interstellar medium reveals that sulfur is near cosmic abundance (*14*, *15*); however, molecular clouds such as TMC-1 and L183 show gas-phase depletions by up to two orders of magnitude (*16*). Astronomers have suggested that gas-grain collisions of ions like singly ionized sulfur (S^+) result in recombination on grain surfaces effectively sequestering the material in neutral forms (*12*). Alternatively, gas-phase sulfur-bearing species such as sulfur dioxide (SO_2) and carbonyl sulfide (OCS) can condense resulting in icy mantles of interstellar grains doped with sulfur (*17*–*20*). During the gravitational collapse of a molecular cloud and transformation to star-forming regions, sublimation should increase observable sulfur in the gas phase. However, observations of protoplanetary disks consistently reveal sulfur depletion at temperatures above the water sublimation threshold of 160 K, suggesting that sulfur may remain locked in refractory molecules on these grain surfaces (*13*)—molecules which have yet to be identified.

Since the organics on Ryugu partially resemble those of presolar grains (*2*), the chemical processes occurring on the icy mantles of grain surfaces likely represent a starting point for sulfur allotrope formation. This pathway could provide insights into the mechanisms of sulfur depletion and illuminate the complex chemistry that shaped Ryugu during its earliest stages of formation. The James Webb Space Telescope has revealed sulfur dioxide (SO_2) (*20*–*22*) as one of the main reservoirs of interstellar sulfur on grain surfaces. Recently, hydrogen sulfide (H_2S) has been suggested as an additional major sulfur sink on grains bolstered via its detection on returned samples from the carbonaceous asteroid Bennu (*23*, *24*). These molecules offer a chemical network for understanding sulfur chemistry in dense clouds. The exposure of sulfur-bearing ices to ionizing radiation afforded several theories on the nature of the refractory sulfur material on the surface of grains including sulfur allotropes (S_n, $n = 2$ to 8) (*25*–*27*), polysulfanes (H_2S_n, $n \geq 2$) (*25*, *26*, *28*), sulfide minerals [iron(II)sulfide, FeS] (*13*), and organosulfur material such as alkylsulfonic acids (R-SO_3H, where R is an alkyl group) (*29*, *30*). Among these variety of selections, cyclic octasulfur (S_8) has sparked intense interest due to its thermodynamic stability and high sublimation temperature (>300 K) (*27*, *31*, *32*). Astrochemical modeling hypothesized that octasulfur (S_8) could represent a notable molecular component in processed interstellar ices (*27*).

Here, we present compelling evidence on the detection of the crown conformer of octasulfur (S_8) along with two sulfur allotropes (S_6 and S_7) synthesized by energetic processing of interstellar analog ices containing sulfur dioxide (SO_2) and hydrogen sulfide (H_2S) under hydrous and anhydrous conditions in laboratory simulation experiments

[1]Department of Chemistry, University of Hawai'i at Mānoa, Honolulu, HI 96822, USA. [2]W. M. Keck Laboratory in Astrochemistry, University of Hawai'i at Mānoa, Honolulu, HI 96822, USA.
*Corresponding author. Email: ralfk@hawaii.edu

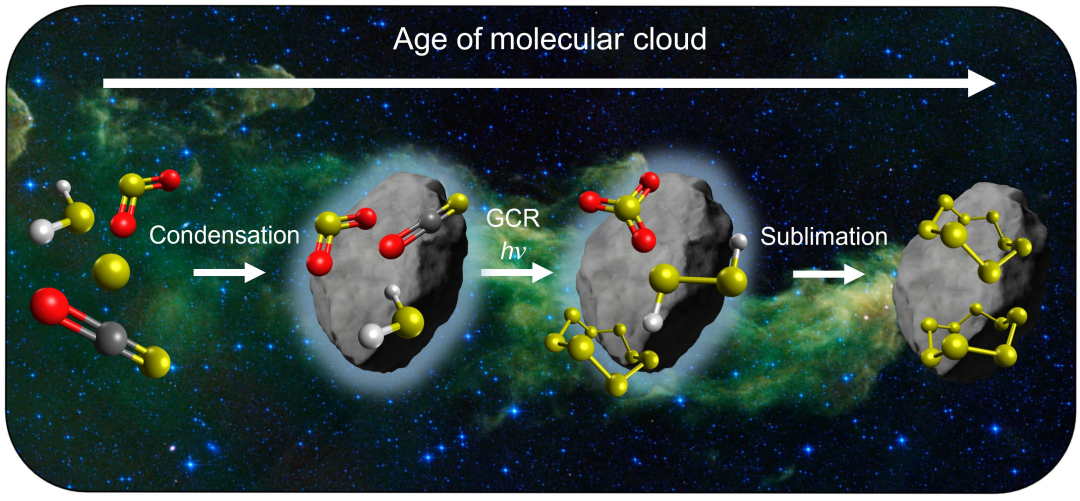

Fig. 1. Proposed routes of sulfur-bearing material in the ISM. Known interstellar sulfur-bearing material exhibits connectivity between sulfur (yellow), oxygen (red), carbon (gray), and hydrogen (white), to form sulfur dioxide (SO_2), hydrogen sulfide (H_2S), and OCS. These compounds remain on interstellar grain surfaces and act as key precursors to larger, complex molecules via ionizing radiation. Background image courtesy NASA/JPL-Caltech.

(table S1). At temperatures relevant to ices on nanoparticles in cold molecular clouds and processed by proxies of GCRs, the cyclic crown conformer of octasulfur (S_8 and D_{4d}) (Fig. 2, **a**) is identified isomer selectively in all sulfur-bearing ices exploiting vacuum ultraviolet (VUV) photoionization reflectron time-of-flight mass spectrometry (PI-ReToF-MS) supported by isotopic analysis of sulfur. The production of octasulfur (S_8) along with two sulfur allotropes (S_7 and S_6) preferentially in hydrogen sulfide (H_2S) doped ices suggests that these allotropes found on Ryugu likely originated from interstellar icy grain mantles and could represent chemical processes akin to the earliest stages of the Solar System.

RESULTS

Fourier transform infrared spectroscopy

Fourier transform infrared (FTIR) spectroscopy was used to monitor the chemical changes triggered by the energetic processing in the ices (SO_2; SO_2/H_2O; SO_2/H_2S; H_2S/H_2O); FTIR spectra were collected before, during, and after the irradiation at 5 K (figs. S1 to S4 and tables S2 to S5). In the pristine ices, prominent vibrational modes of SO_2 such as ν_1 (1146 cm^{-1}) (*22*), ν_3 (1310–1343 cm^{-1}) (*22*) in SO_2, SO_2/H_2O, and SO_2/H_2S ices are visible. Fundamentals of H_2O such as ν_1/ν_3 (3000 to 3500 cm^{-1}) (*33*), ν_2 (1650 cm^{-1}) (*33*), and lattice modes (ν_L, 811 cm^{-1}) (*33*) were found in water-containing ices (figs. S2 and S4), while H_2S was detected via the ν_3 (2596 cm^{-1}) (*34*), ν_1 (2557 cm^{-1}) (*34*), and ν_2 (1171 cm^{-1}) (*34*) modes in the SO_2/H_2S (fig. S3) and H_2S/H_2O (fig. S4) ices. After the energetic processing, the FTIR spectra were deconvoluted to assign emerging new features to the functional groups. Sulfur trioxide (SO_3, ν_3, 1388 cm^{-1}) (*35*) was detected in the SO_2 ice; S—H stretching vibration associated with polysulfanes (H_2S_n, 2488 cm^{-1}) (*36*, *37*) could be traced in the hydrogen sulfide ices. Multiple vibrations assigned to S═O stretching modes (1300 to 1089 cm^{-1}) (*38*) are observed in the SO_2/H_2O and SO_2/H_2S experiments along with the S—O stretching mode (1049 to 806 cm^{-1}) (*38*); O—H stretching modes are visible at (2931 to 2141 cm^{-1}) (*38*). The emergence of new O—H stretching, S—O stretching, and S═O stretching may indicate the formation of inorganic acids such as H_2SO_3 and H_2SO_4. Although FTIR spectroscopy represents an ideal tool in the elucidation of the emergence of functional groups, the identification of discrete molecules such as sulfanes (H_2S_n; $n > 2$) and sulfur (S_8) is problematic due to overlapping vibrations modes, infrared inactive vibrations, and/or infrared active modes outside the range of the mid-FTIR (<500 cm^{-1}). Therefore, to unambiguously identify sulfur (S_8), an alternative analytical approach is clearly required.

Photoionization reflectron time-of-flight mass spectrometry

PI-ReToF-MS was exploited to identify isomer-specific reaction products based on the desorption temperatures and adiabatic ionization energies (IEs) (Fig. 2 and table S6) (*39*, *40*). The detection of sulfur (S_8) represents the overarching goal of this project. Previous electronic structure calculations in the work by Herath *et al.* (*41*) reveals six conformers and isomers of octasulfur (S_8; Fig. 2, **a** to **f**) with IEs between 8.90 and 8.15 eV. These calculations were conducted using the CCSD(T)-F12b/cc-pVTZ-F12//B3LYP/aug-cc-pVTZ level of theory—using MOLPRO 2024.1 (*42*, *43*) and Gaussian16 (*44*)—which is well known to produce accurate and precise adiabatic IE calculations within an error of ± 0.05 eV and sometimes as low as 0.01 eV (*45*–*47*). Two VUV photon energies were used (table S7). At 9.34 eV, all conformers and isomers of S_8 (**a** to **f**) can be ionized, while at 8.75 eV, all species except the crown conformer **a** can be ionized. During the temperature-programmed desorption (TPD), newly formed molecules that sublime, are subsequently photoionized by pulsed VUV light and detected via ReToF-MS. Figure 3 compiles the overall ion counts from mass-to-charge ratio (m/z) 1 to 400 during TPD collected at 9.34 eV. It should be highlighted that this soft photoionization does not produce dications, thus resulting in m/z values equivalent to the molecular mass of the product (unified atomic mass unit).

SO_2 ice

The most intense ion counts correspond to $m/z = 256$ at 258 K. This value matches the molecular mass of S_8 of $m/z = 256$ with eight ^{32}S (Fig. 4). Considering natural isotopic abundances of sulfur, particularly ^{33}S and ^{34}S, the number of sulfur atoms can be determined on the basis of the mass distribution across isotopolog channels (Fig. 5).

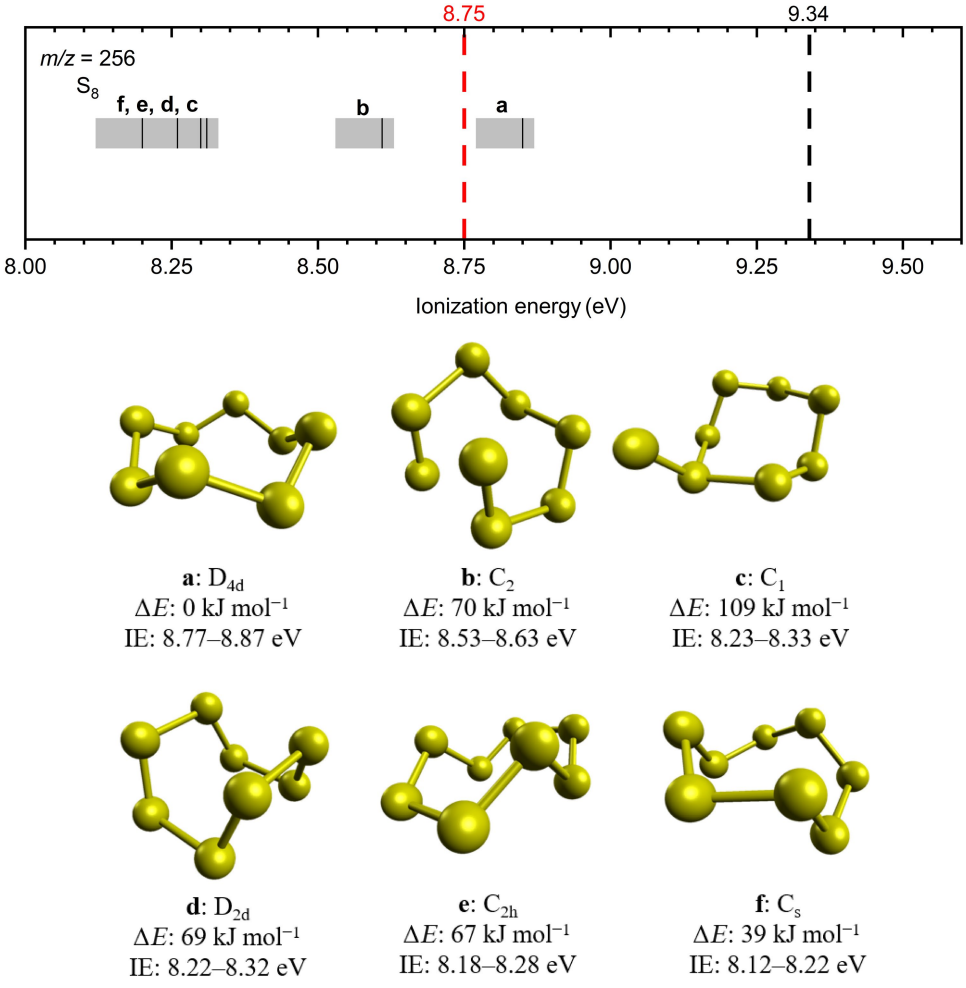

Fig. 2. Compilation of computed adiabatic IEs of S_8 isomers/conformers (black solid lines), IE ranges (gray area) after error analysis, and relative energy (Δ*E*). Point groups of S_8 conformers are shown. IEs are calculated with the CCSD(T)-F12b/cc-pVTZ-F12//B3LYP/aug-cc-pVTZ level of theory in (*41*) including zero-point vibrational energy corrections. VUV photon energies at 9.34 and 8.75 eV (dashed lines) were chosen to selectively ionize subliming species during TPD.

S_8 should exhibit *m/z* signal ratios at 256:258:260 of 17.6:6.3:1. In contrast, a molecule such as S_7O_2 (*m*/z = 256) would yield a ratio of 22.6:7.2:1. By comparing the observed ion count values to these reference ratios, an effective isotopic ratio is determined. Our experimentally derived ratio for *m/z* = 256:258:260 is 17.6:6.3:1 matching exceptionally well for S_8. At 8.75 eV, these ion counts disappear, suggesting that the adiabatic IE of the isomer or conformer exceeds 8.75 eV. This confirms the presence of only the crown conformer of S_8 (**a**). In addition, a smaller peak with *m/z* = 224 appears at 312 K (fig. S5). Similar to S_8, heptasulfur (S_7) was confirmed through isotopic distribution analysis of the *m/z* of 224 (S_7):226 ($S_6{}^{34}S$), revealing a 3.4:1 ratio close to the theoretical ratio of 3.23:1.

SO_2/H_2O ice

Unlike the pure SO_2 ice, the SO_2/H_2O experiments reveal additional products. Sulfane (H_2S_n) production is well defined in this ice (fig. S6) revealing signals corresponding to H_2S_2 (*m/z* = 66; IE = 9.3 eV) (*48*), H_2S_3 (*m/z* = 98; IE = 8.7 to 9.27), H_2S_4 (*m/z* = 130; IE = 6.77 to 8.82), H_2S_5 (*m/z* = 162; IE = 8.56 to 8.71), H_2S_6 (*m/z* = 194; IE = 8.50 to 8.90), and H_2S_7 (*m/z* = 226; IE = 8.43 to 8.78). Similar to the SO_2 experiment, S_7 (*m/z* = 224) exhibits a sublimation peak at 312 K. Three peaks are observed for S_8. Peak **1** (Fig. 4) shows too few counts to quantify the isotopic distribution to confirm S_8. Peaks **2** and **3** depict isotopic distributions matching those of octasulfur (S_8) with ratios at 256:258:260 of 16:6:1 for both peaks. The origin of these three peaks may be due to the sublimation of different products in the ice matrix. For instance, peak **1** shows cosublimation with H_2S_5 (*m/z* = 162; 240 K), while peak **2** cosublimes with H_2S_6 (*m/z* = 194; 270 K) (fig. S5). Furthermore, the disappearance of these peaks in the 8.75 eV experiments confirms the crown conformer of octasulfur (S_8) **a**.

H_2S/H_2O ice

Sulfane production is a key feature of irradiated H_2S containing ices. Here, the formation of H_2S_2 (*m/z* = 66), H_2S_3 (*m/z* = 98), H_2S_4 (*m/z* = 130), H_2S_5 (*m/z* = 162), H_2S_6 (*m/z* = 194), H_2S_7 (226 *m/z*), H_2S_8 (258 *m/z*), H_2S_9 (290 *m/z*), H_2S_{10} (322 *m/z*), and H_2S_{11} (354 *m/z*) is evident (fig. S8). In addition, sulfur molecules such as S_6 (*m/z* = 192) and S_7 (*m/z* = 224) (figs. S9 and S10) were formed during the radiation exposure. Hexasulfur (S_6) was confirmed by normalizing

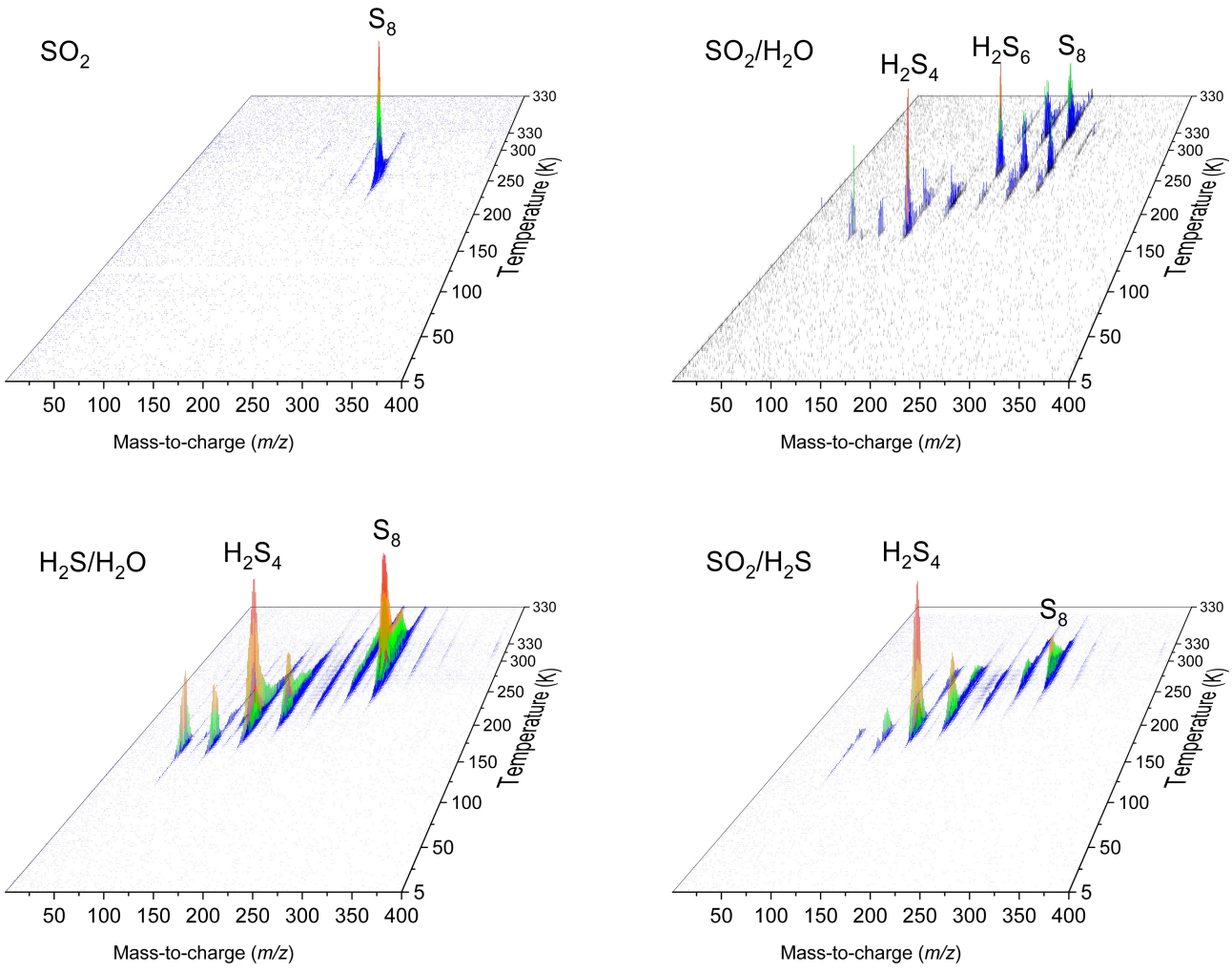

Fig. 3. PI-ReToF-MS data of the irradiated SO_2 ice, SO_2/H_2O ice, H_2S/H_2O ice, and SO_2/H_2S ice recorded using 9.34 eV photons during TPD. Ion counts measured by the ReToF-MS of all recorded masses (m/z = 1 to 400) were recorded during TPD from 5 to 330 K and held until all signals returned to baseline.

and subtracting the signal of H_2S_7 (m/z = 226) from m/z = 192, which is known to fragment to S_6 (*41*). After correction, the isotopolog of m/z = 194 (primarily $^{34}S^{32}S_5$) was compared with m/z = 192 ($^{32}S_6$), giving a calculated ratio of 192:194 of 3.9:1, resembling the expected theoretical ratio of 3.7:1. Heptasulfur (S_7) can be confirmed by isotopic distribution of the m/z of 224:226 of 3.2:1 matching the expected isotopic distribution pattern exceptionally well (3.23:1). At m/z = 256, two sublimation events are detected. Peak **1** (Fig. 4, H_2S/H_2O) has a mass to charge distribution ratio for 256:258:260 of 12:5:1 and hence cannot be connected to octasulfur (S_8) but rather cosublimation or fragmentation of H_2S_8. Fragmentation of higher-order sulfanes is evidenced by the photon energy–dependent behavior of the mass signals (fig. S11) and has been reported previously (*41*). Upon tuning the photon energy to 8.75 eV, the signal at m/z = 258 (H_2S_8) is maintained and temporally coincides with peak **1**. It should be noted that no signal at 8.75 eV is observed for S_8, suggesting that the signal for m/z = 258 cannot derive from $S_7{}^{34}S$ but instead from H_2S_8. The temporal overlap and the matching peak shape suggest that fragmentation of H_2S_8 could contribute to the signal in m/z = 256 (S_8^+). In contrast, peak **2** can be confirmed to be octasulfur (S_8) given its isotopic distribution ratios of 15:6:1 for m/z = 256:258:260. As is the previously analyzed ices, the signal is not detected for 8.75 eV photons confirming the crown conformer of octasulfur (S_8) **a**.

SO_2/H_2S ice

Similar to the H_2S/H_2O ice, two distinct peaks are observed in the TPD profile for m/z = 256 sublimation of octasulfur (S_8). Peak **1** (Fig. 4) originates from fragmentation of higher order sulfanes (e.g., H_2S_8) (fig. S12), while peak **2** corresponds to the sublimation of octasulfur (S_8). Similar to the H_2S/H_2O ices, fragmentation of H_2S_8 (fig. S13) is revealed by photon energy–dependent ionization. At 8.75 eV, the H_2S_8 parent ion is observed without formation of S_8, and this sublimation of H_2S_8 coincides with peak **1**, indicating that the fragmentation of sulfanes, e.g., H_2S_8, contributes to the signal in m/z = 256 at peak **1**. In addition, peak **1** contains an isotopic distribution of 13:5:1 suggesting enrichment of the isotopolog channels (m/z = 258 and 260) and thus cannot be definitively confirmed to be solely S_8. Peak **2** shows an isotopic distribution of 17:6:1 for m/z = 256:258:260 resembling that of S_8. At a photon energy of 9.34 eV, both peaks are visible, whereas at 8.75 eV, the signal disappears. Since peak **1** cannot be

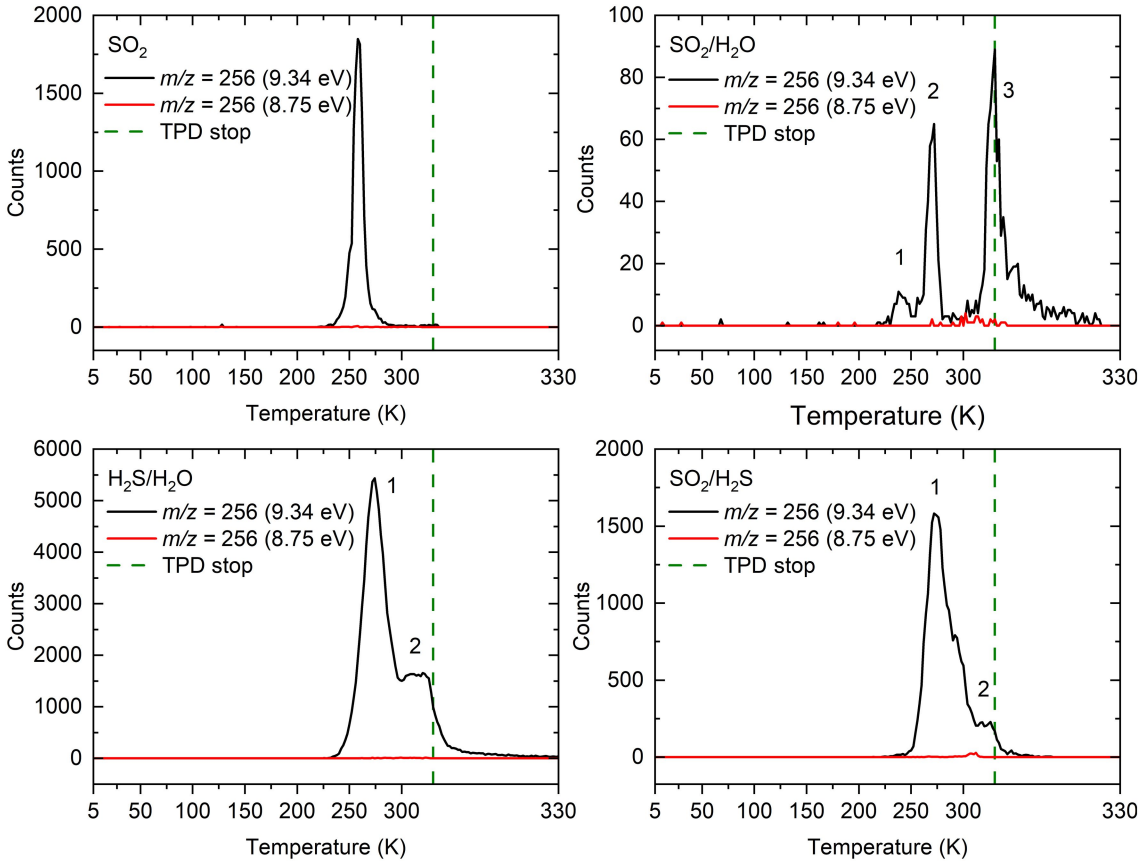

Fig. 4. TPD-ReToF-MS profiles of each sulfur-bearing ice after processing by energetic electrons (100 nA, 1 hour). Ion counts measured by the ReToF-MS of the 256 *m/z* channel during TPD (5 to 330 K) with photon energies of 9.34 eV (black) and 8.75 eV (red). Once the TPD was finished at 330 K (green dashed), the temperature of the substrate was held until the signal returned to baseline.

directly tied to S_8 due to a mismatch in isotopic distribution to S_8, only peak **2** can be confirmed for the crown conformer **a** of S_8. In addition, a series of sulfanes from H_2S_2 to H_2S_{10} (fig. S12) is detected during TPD along with sulfur allotropes such as S_6 and S_7 (fig. S14). Because of low counts in the S_6 ($m/z = 192$) mass spectrum after fragmentation correction of H_2S_7, S_6 can only be tentatively assigned.

DISCUSSION

Since we confirm the presence of octasulfur in the crown conformer **a** of S_8, we can quantify the production yields and production efficiency using the photoionization cross section of S_8 (**a**) at 9.34 eV ($3.4 \pm 2.0 \times 10^{-17}$ cm^2) (*41*); the detailed process to compute the yields and production efficiencies is outlined in Materials and Methods. Each ice experiment shows varying degrees of production of cyclic octasulfur (**a**)—hereafter S_8 (Table 1)—with the H_2S/H_2O experiment unexpectedly revealing the most efficient formation across all experiments with a conversion yield of $8.4 \pm 4.8 \times 10^{-4}$ molecules eV^{-1}. In contrast, the SO_2/H_2O ice has a yield of $3.4 \pm 2.0 \times 10^{-5}$ molecules eV^{-1}, which suggests that the sulfur (+IV) oxidation state in sulfur dioxide may resist reduction in water ices to S(0) in S_8. Previous studies have shown that sulfur dioxide may further oxidize in interstellar analog ices to form sulfur trioxide (SO_3) (*30*, *35*, *49*, *50*) and sulfuric acid (H_2SO_4) (*30*, *50*); likewise, reaction with water yields sulfurous acid (H_2SO_3) (*50*) and the sulfonic acid functional group (-SO_3H) (*30*). The contrast between the S_8 production in H_2S/H_2O and SO_2/H_2O ices specifically points to the ease for S(−II) in hydrogen sulfide (H_2S) to oxidize to neutral sulfur such as in cyclic octasulfur than the reduction of S(+IV) in sulfur dioxide (SO_2).

The percentage yield of S_8 in SO_2/H_2S ices ($2.9 \pm 1.7\%$) closely resembles the yield in SO_2/H_2O ices ($1.6 \pm 0.9\%$), whereas H_2S/H_2O ices ($27.0 \pm 16\%$) do not. Further, the addition of water in the H_2S experiments enhances the production yield of S_8 ($27.0 \pm 16\%$) over anhydrous conditions ($3.4 \pm 0.4\%$) (*41*). In the hydrous network, hydrogen sulfide seems to resist oxidation past neutral sulfur [S(0)], contrary to well-known processes occurring in water ices (*51*). This could indicate that acid formation (H_2SO_3 and H_2SO_4) likely derives from SO_2 on icy interstellar grains rather than from H_2S.

Contrary to H_2S, the SO_2/H_2O reveals the resistance of SO_2 to convert to S_8. Recent detections from Ryugu asteroid extracts suggest that the sulfonic acid functional group, as observed in polythionic acids (HO_3S-S_n-SO_3H; $n < 6$) (*1*), may "cap" sulfur chains thus limiting their growth. The generation of these end groups could be a key factor in restricting sulfur chain growth and, consequently, S_8 production. Moreover, this indicates that SO_2 is likely not a primary contributor to S_8, but rather H_2S plays a dominant role in the synthesis of sulfur allotropes like S_8 on interstellar grains. Thus, S_8 formation is highly dependent on the oxidation state of sulfur in the

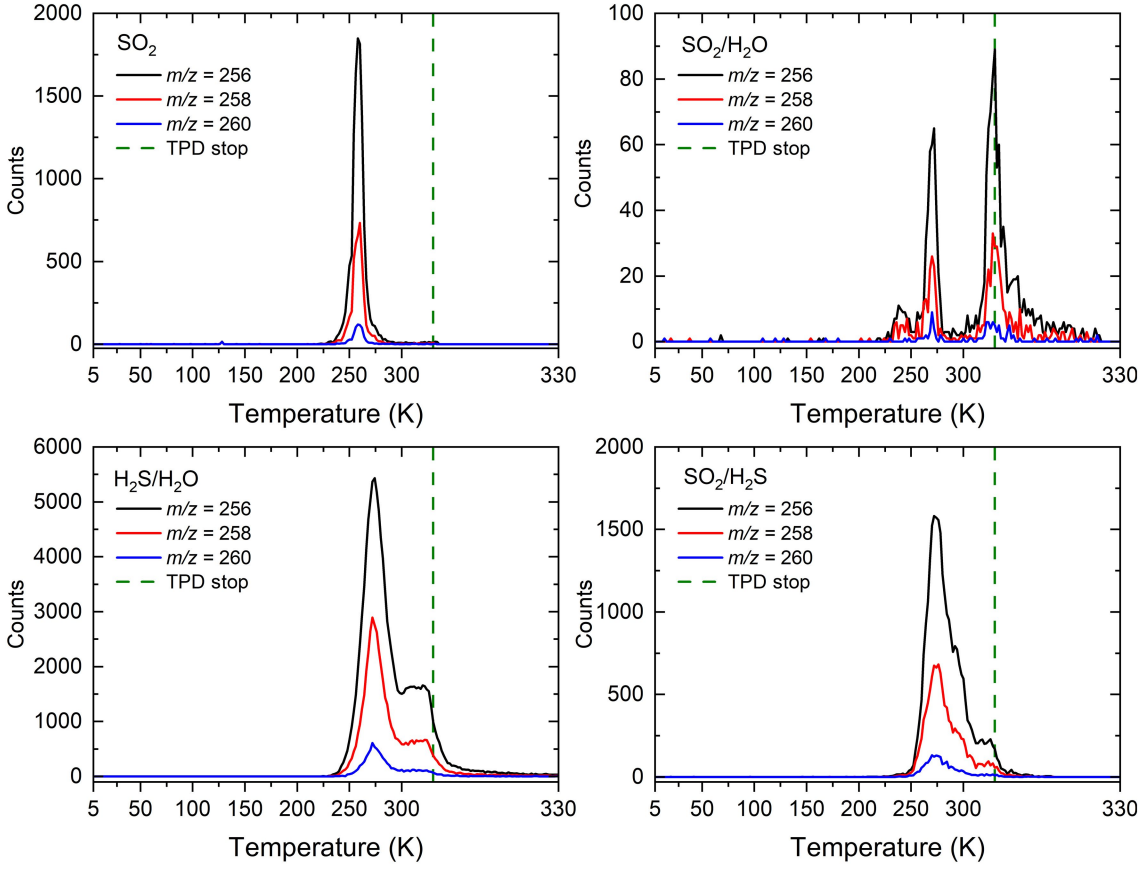

Fig. 5. TPD-ReToF-MS profiles of each sulfur-bearing ice after processing by energetic electrons (100 nA, 1 hour). Ion counts measured by the ReToF-MS using a photon energy of 9.34 eV. The mass channel $m/z = 256$ correlates to S_8, and the other mass channels—$m/z = 258$ and 260—correspond to different isotopologs of S_8. Once the TPD was finished at 330 K (green dashed), the temperature of the substrate was held until the signal returned to baseline.

Table 1. Calculated conversion yields of reagent material to S_8 in the experiments. The percent yield of S_8 was determined on the basis of the number of sulfur atoms within the maximum electron penetration depth of each ice mixture (see table S9). The total number of S_8 molecules detected by ReToF-MS, combined with the radiation dose calculated using CASINO v2.42 software suite, was used to determine the conversion yield for each ice. Additional details are provided in the Supplementary Materials.

Ice	Available sulfur atoms	S_8 produced (molecule)	Percent yield	Conversion yield (molecule eV^{-1})	Reference
H_2S	–	–	3.4 ± 0.4	$6.8 \pm 1.0 \times 10^{-4}$	(*41*)
SO_2	5.8×10^{17}	$1.8 \pm 1.0 \times 10^{15}$	5.0 ± 2.9	$3.2 \pm 1.8 \times 10^{-4}$	This work
H_2S/H_2O	2.8×10^{17}	$4.8 \pm 2.7 \times 10^{15}$	27 ± 16	$8.4 \pm 4.8 \times 10^{-4}$	This work
SO_2/H_2O	1.9×10^{17}	$1.9 \pm 1.1 \times 10^{14}$	1.6 ± 0.9	$3.4 \pm 2.0 \times 10^{-5}$	This work
SO_2/H_2S	7.5×10^{17}	$1.4 \pm 0.7 \times 10^{14}$	2.9 ± 1.7	$2.5 \pm 1.4 \times 10^{-4}$	This work

precursors in the ices and suggests the resistance of the S═O bonds to cleavage with higher SO_2:H_2S ratios suppressing the growth of larger sulfur allotropes.

To understand possible mechanisms through oxidation and reduction of H_2S and SO_2, respectively, we analyze the barriers and energetics to form sulfur allotropes in both cases. Upon interaction with energetic electrons, cleavage of the reagent material (SO_2 or H_2S) can produce reactive radicals along with suprathermal atoms initiating nonequilibrium chemical reactions (*52*, *53*). For sulfur chain growth to occur, a source of sulfur atoms is required. Upon interaction with energetic electrons, SO_2 can endoergically produce molecular oxygen (O_2; $^3\Sigma_g^-$) and atomic sulfur (S; ^3P) (reaction 1). This process can be also replaced by a two-step reaction via sulfur monoxide (SO) (reactions 2 and 3), for which two oxygen atoms are cleaved step wise.

$$SO_2 \rightarrow S(^3P) + O_2(X^3\Sigma_g^-) \qquad \Delta_R G = +571 \text{ kJ mol}^{-1} \quad (1)$$

$$SO_2 \rightarrow O(^3P) + SO\ (X^3\Sigma_g^-) \quad \Delta_R G = +547\ \text{kJ mol}^{-1} \quad (2)$$

$$SO \rightarrow O(^3P) + S\ (^3P) \quad \Delta_R G = +518\ \text{kJ mol}^{-1} \quad (3)$$

In the case of H_2S, sulfur atoms can be produced similarly to reaction 1, where both hydrogen-sulfur bonds are broken to produce molecular hydrogen (H_2) and atomic sulfur (reaction 4) (*7*). Similar to SO_2, this can be described by a two-step process where H_2S loses one hydrogen atom to form the sulfanyl radical (SH) and again to produce atomic sulfur (reactions 5 and 6).

$$H_2S \rightarrow S(^1D) + H_2\ (X^1\Sigma_g^+) \quad \Delta_R G = +405\ \text{kJ mol}^{-1} \quad (4)$$

$$H_2S \rightarrow H(^2S) + SH\ (X^2\Pi_{3/2}) \quad \Delta_R G = +376\ \text{kJ mol}^{-1} \quad (5)$$

$$SH \rightarrow S(^3P) + H\ (^2S) \quad \Delta_R G = +350\ \text{kJ mol}^{-1} \quad (6)$$

Comparing the conversion in one step shows that the formation of atomic sulfur in SO_2 is more endoergic compared to H_2S by 166 kJ mol^{-1}, while the two-step process pushes this difference to 339 kJ mol^{-1} exemplifying the stability of the S═O bond. This relative difference in reaction energetics illustrates that H_2S—under irradiated conditions—is likely favored in producing sulfur atoms over SO_2. The necessity of sulfur atom production between SO_2 and H_2S correlates to sulfur chain growth in the ices where H_2S shows the most signal in all polysulfane and allotrope (S_6, S_7, and S_8) mass channels. After formation of atomic sulfur, subsequent barrierless radical-radical recombination of sulfur atoms (S; ^3P) can produce disulfur (S_2; $X\ ^3\Sigma_g^-$) (reaction 7).

$$S\ (^3P) + S\ (^3P) \rightarrow S_2\ (X^3\Sigma_g^-) \quad \Delta_R G = -426\ \text{kJ mol}^{-1} \quad (7)$$

Disulfur being a diradical allows for subsequent radical-radical recombination with atomic sulfur (^3P) to form trisulfur ($\Delta_R G = -260$ kJ mol^{-1}) (*54*) (reaction 8). This reaction scheme can be repeated via radical-neutral addition to form tetrasulfur (S_4; $\Delta_R G = -198$ kJ mol^{-1}) (reaction 9) (*54*).

$$S_2\ (X^3\Sigma_g^-) + S\ (^3P) \rightarrow S_3\ (X^1A_1) \quad \Delta_R G = -260\ \text{kJ mol}^{-1} \quad (8)$$

$$S_3\ (X^1A_1) + S\ (^3P) \rightarrow S_4\ (X^1A_1) \quad \Delta_R G = -198\ \text{kJ mol}^{-1} \quad (9)$$

Since S_3 is a singlet ground state and atomic sulfur has a triplet ground state, this process is governed by nonadiabatic dynamics to produce the ground-state singlet tetrasulfur (S_4; X^1A_1). Both reactions are exoergic and, upon sulfur addition, can continue to form S_5, S_6, S_7, and S_8. The relative stability of these species is well known with S_8 being particularly stable and accounting for 99% of elemental sulfur in terrestrial environments. Thus, the absence of smaller allotropes (S_2 to S_5) could be due to relative stability of each species.

Alternatively, reactions between highly reactive, small sulfur molecules may produce S_8. Disulfur films on a solid surface reveal no barrier in radical-radical recombination forming tetrasulfur (reaction 10) (*55*, *56*). Theoretical calculations have indicated disulfur self-reactions are barrierless and exoergic 96 kJ mol^{-1}, indicating that small sulfur allotropes can produce larger material spontaneously (*57*, *58*).

$$S_2\ (X^3\Sigma_g^-) + S_2\ (X^3\Sigma_g^-) \rightarrow S_4\ (X^1A_1) \quad \Delta_R G = -96\ \text{kJ mol}^{-1} \quad (10)$$

Subsequently, neutral-neutral reactions of tetrasulfur could generate octasulfur (reaction (11). Ab initio calculations show that this reaction is exoergic by 345 kJ mol^{-1} at the ωB97X-D/cc-pVTZ level of theory (*59*).

$$S_4\ (X^1A_1) + S_4\ (X^1A_1) \rightarrow S_8\ (X^1A_1) \quad \Delta_R G = -345\ \text{kJ mol}^{-1} \quad (11)$$

The lack of S_2 and S_5 in these ices are likely due to high reactivity of sulfur allotropes, thus if they are formed, the sulfur allotropes quickly undergo further nonequilibrium reactions. The relative stability of sulfur allotropes is well known, with ring conformers of S_6, S_7, and S_8 being more stable than sulfur chains (*60*).

Once formed within the icy mantles of interstellar grains, sulfur allotropes such as S_6, S_7, and S_8 can remain in refractory form, effectively sequestering sulfur into the condensed phase. The condensation of gaseous sulfur onto interstellar grains, followed by alteration through GCRs, facilitates the transformation of sulfur into refractory species. These forms are resistant to thermal processing during the gravitational collapse of molecular clouds, thereby diminishing the abundance of detectable gas-phase sulfur. Notably, allotropes like S_8 exhibit resistance to sublimation at temperatures up to 300 K, supporting their role as a viable mechanism for sulfur depletion in molecular clouds.

Since the organics found on Ryugu resemble those formed on presolar grains (*2*), our results detail a formation scenario where refractory sulfur allotropes are formed in interstellar ices before incorporation into Ryugu. Thus, the inventory of Ryugu at least partially derives from interstellar icy mantles doped with sulfur species like SO_2 and H_2S and can be effectively reproduced via condensed-phase nonequilibrium chemical reactions. Although hydrogen sulfide has yet to be detected on grain surfaces—likely due to weak infrared band strengths—the chemistry from grains indicates that allotropes derive from H_2S rather than SO_2 in these hydrous environments. In addition, the presence of oxidized species such as sulfur trioxide (SO_3), sulfurous acid (H_2SO_3), and sulfuric acid (H_2SO_4) in the SO_2/H_2O ices but not in the H_2S/H_2O ices indicates that these highly oxidized species correlate to SO_2. Moreover, these sulfur species could be precursors to other sulfur material found in Ryugu such as polythionic acids (HO_3S-S_n-SO_3H; $n < 6$). Specifically, H_2SO_3 and SO_3 both correlate to the -SO_3H functional group of polythionic acids. Once the addition of the -SO_3H functional group occurs, the sulfur chain cannot proceed to sulfur ring formation (S_6, S_7, and S_8).

Here, the unambiguous identification of the crown conformer (**a**) of octasulfur (S_8) along with hexasulfur (S_6) and heptasulfur (S_7) allotropes in hydrous sulfur-doped ices establishes hydrogen sulfide (H_2S) as the dominant source of sulfur allotropes on interstellar grains. This synthesis proceeds likely via sulfur chain growth and possibly via reactions between small sulfur allotropes upon exposure of sulfur-containing material to proxies of GCRs. The identification of S_6, S_7, and S_8 in various mixed ices provides compelling evidence for the limitations of allotrope production and reveals a resistance to reduction of S(+IV) in sulfur dioxide (SO_2) but facile oxidation of S(−II) in hydrogen sulfide (H_2S) in interstellar icy mantles. In addition, our works highlight plausible mechanistic details about side product formation and sulfur chain capping in interstellar ices

linking them to refractory material such as hexasulfur (S_6), heptasulfur (S_7), and octasulfur (S_8) as found in the carbonaceous asteroid Ryugu. This suggests sulfur dioxide as a likely contributor to polythionic acids and hydrogen sulfide as the primary reagent in allotrope formation. These results link icy mantles of presolar grains to material found in Ryugu. Besides our Solar System, the production of higher-order allotropes presents a plausible sulfur depletion mechanism in interstellar grains. Our results indicate that S_6, S_7, and S_8 are common material in sulfur-containing ices upon exposure to irradiation, with S_8 being the most abundant allotrope. Understanding these formation processes is crucial for developing a mechanistic network for sulfur depletion in molecular clouds and expands our fundamental knowledge of sulfur chemistry on interstellar grain surfaces with broader implications into the chemistry of small celestial bodies like carbonaceous asteroids Ryugu and the earliest stages of our Solar System.

MATERIALS AND METHODS

All experiments used an ultrahigh vacuum (UHV) stainless steel chamber held at pressures of 5×10^{-11} torr by magnetically levitated turbo molecular pumps (Osaka, TG1300MUCWB, TG420MCAB) backed by an oil-free dry scroll pump (XDS35i, Edwards). A mirror-finished silver substrate was attached to a cold head and cooled to 5 K by a closed-cycle helium refrigerator (Sumitomo Heavy Industries, RDK-415E). Reagent materials—SO_2 (Matheson, 99.98%), H_2S (Sigma-Aldrich, 99.9%), and water (Honeywell, high-performance liquid chromatography grade)—were introduced through separate glass capillary arrays into the UHV chamber and deposited on the substrate at 5 K. The gas deposition was monitored using interferometry by a HeNe laser (Melles Griot, 25-LHP-230, 632.8 nm) (*61*). A refractive index of each ice mixture was calculated on the basis of the average refractive index of each ice reagent SO_2 ($n = 1.33$) (*62*), H_2S ($n = 1.41$) (*63*), and H_2O ($n = 1.27$) (*64*) and was exploited to calculate the ice thickness (table S1). An FTIR spectrometer (Thermo Fisher Scientific, Nicolet 6700) with a range of 6000 to 500 cm^{-1} and a resolution of 4 cm^{-1} was used to determine the reagent ratio in the ices based on their respective band strengths (table S8).

After deposition, the ice mixtures were irradiated using 5 keV electrons produced from an electron gun (SPECS, EQ PU-22) scanning over an area of 1.6 cm^2 at 100 nA of current for 60 min. These doses simulate secondary electrons generated by GCRs in cold molecular clouds up to an age of 2×10^7 years (*65*). The average penetration depth and doses per molecule of each ice can be found in table S9. These calculations are derived from Monte Carlo simulations using CASINO v2.42 software suite (*66*). The maximum penetration depth was found to be less than the ice thickness in all experiments, suggesting that all reactions are from the ice and the electrons do not interact with the silver substrate.

After irradiation, the ices were heated from 5 to 320 K at 1 K min^{-1} to facilitate sublimation of material from the surface in a TPD process. The TPD phase simulates the increase of temperature during molecular cloud collapse to star-forming regions (*67*). Subliming molecules were photoionized by pulsed VUV light (30 Hz), which was generated through resonant four-wave mixing schemes inside a noble gas jet pumped by two tunable dye lasers (Sirah, Cobra-Stretch) each pumped by an Nd:YAG laser (Spectra Physics, Quanta Ray Pro 250-30 and 270-30) (*68*, *69*). Dyes and wavelengths used in the generation of VUV light can be found in table S7. The VUV light was separated from other laser light using a lithium fluoride lens in an off-axis geometry. Ionized molecules were detected by a dual microchannel plate using a reflectron time-of-flight mass spectrometer (Jordan TOF Products). Signals generated by the ions were amplified with a preamplifier (Ortec 9305) and recorded with a multichannel scaler (FAST ComTec, MCS6A). Each mass spectrum used an accumulation time of 2 min (3600 sweeps) and an arrival time accuracy of 3.2 ns. To quantify the amount of octasulfur produced in each ice, the reflectron time-of-flight mass spectrometer was calibrated by using an experiment that ionizes both H_2S and S_8 at 10.49 eV along with the respective photoionization cross sections (*41*). For more information on the quantification of octasulfur, see the Supplementary Materials.

Supplementary Materials

This PDF file includes:

Supplementary Text
Tables S1 to S9
Figs. S1 to S18
References

REFERENCES

1. T. Yoshimura, Y. Takano, H. Naraoka, T. Koga, D. Araoka, N. O. Ogawa, P. Schmitt-Kopplin, N. Hertkorn, Y. Oba, J. P. Dworkin, J. C. Aponte, T. Yoshikawa, S. Tanaka, N. Ohkouchi, M. Hashiguchi, H. McLain, E. T. Parker, S. Sakai, M. Yamaguchi, T. Suzuki, T. Yokoyama, H. Yurimoto, T. Nakamura, T. Noguchi, Hayabusa2-initial-analysis SOM team, Chemical evolution of primordial salts and organic sulfur molecules in the asteroid 162173 Ryugu. *Nat. Commun.* **14**, 5284 (2023).
2. A. N. Nguyen, P. Mane, L. P. Keller, L. Piani, Y. Abe, J. Aléon, C. M. O. D. Alexander, S. Amari, Y. Amelin, K.-i. Bajo, M. Bizzarro, A. Bouvier, R. W. Carlson, M. Chaussidon, B.-G. Choi, N. Dauphas, A. M. Davis, T. Di Rocco, W. Fujiya, R. Fukai, I. Gautam, M. K. Haba, Y. Hibiya, H. Hidaka, H. Homma, P. Hoppe, G. R. Huss, K. Ichida, T. Iizuka, T. R. Ireland, A. Ishikawa, S. Itoh, N. Kawasaki, N. T. Kita, K. Kitajima, T. Kleine, S. Komatani, A. N. Krot, M.-C. Liu, Y. Masuda, K. D. McKeegan, M. Morita, K. Motomura, F. Moynier, I. Nakai, K. Nagashima, D. Nesvorný, L. Nittler, M. Onose, A. Pack, C. Park, L. Qin, S. S. Russell, N. Sakamoto, M. Schönbächler, L. Tafla, H. Tang, K. Terada, Y. Terada, T. Usui, S. Wada, M. Wadhwa, R. J. Walker, K. Yamashita, Q.-Z. Yin, T. Yokoyama, S. Yoneda, E. D. Young, H. Yui, A.-C. Zhang, T. Nakamura, H. Naraoka, T. Noguchi, R. Okazaki, K. Sakamoto, H. Yabuta, M. Abe, A. Miyazaki, A. Nakato, M. Nishimura, T. Okada, T. Yada, K. Yogata, S. Nakazawa, T. Saiki, S. Tanaka, F. Terui, Y. Tsuda, S.-i. Watanabe, M. Yoshikawa, S. Tachibana, H. Yurimoto, Abundant presolar grains and primordial organics preserved in carbon-rich exogenous clasts in asteroid Ryugu. *Sci. Adv.* **9**, eadh1003 (2023).
3. M. J. Mumma, S. B. Charnley, The chemical composition of comets—Emerging taxonomies and natal heritage. *Annu. Rev. Astron. Astrophys.* **49**, 471–524 (2011).
4. J. R. Cronin, S. Chang, "Organic matter in meteorites: Molecular and isotopic analyses of the murchison meteorite," in *The Chemistry of Life's Origins*, J. M. Greenberg, C. X. Mendoza-Gómez, V. Pirronello, Eds. (Springer Netherlands, 1993), pp. 209–258.
5. M. Tang, S.-L. Qin, T. Liu, L. A. Zapata, X. Liu, Y. Peng, F. Xu, C. Zhang, K. I. Tatematsu, A survey of sulfur-bearing molecular lines toward the dense cores in 11 massive protoclusters. *Astrophys. J. Suppl. Ser.* **275**, 25 (2024).
6. D. V. Mifsud, P. Herczku, R. Ramachandran, P. Sundararajan, K. K. Rahul, S. T. S. Kovács, B. Sulik, Z. Juhász, R. Rácz, S. Biri, Z. Kaňuchová, S. Ioppolo, B. Sivaraman, R. W. McCullough, N. J. Mason, A systematic mid-infrared spectroscopic study of thermally processed H_2S ices. *Spectrochim. Acta A* **319**, 124567 (2024).
7. J. Zhou, Y. Zhao, C. S. Hansen, J. Yang, Y. Chang, Y. Yu, G. Cheng, Z. Chen, Z. He, S. Yu, H. Ding, W. Zhang, G. Wu, D. Dai, C. M. Western, M. N. R. Ashfold, K. Yuan, X. Yang, Ultraviolet photolysis of H_2S and its implications for SH radical production in the interstellar medium. *Nat. Commun.* **11**, 1547 (2020).
8. J. C. Santos, H. Linnartz, K.-J. Chuang, Interaction of H_2S with H atoms on grain surfaces under molecular cloud conditions. *Astron. Astrophys.* **678**, A112 (2023).
9. A. Penzias, P. Solomon, R. Wilson, K. Jefferts, Interstellar carbon monosulfide. *Astrophys. J.* **168**, L53 (1971).
10. M. Oppenheimer, A. Dalgarno, The chemistry of sulfur in interstellar clouds. *Astrophys. J.* **187**, 231–236 (1974).
11. P. M. Gondhalekar, Depletion of sulphur in the interstellar medium. *Mon. Not. R. Astron. Soc.* **217**, 585–588 (1985).
12. D. P. Ruffle, T. W. Hartquist, P. Caselli, D. A. Williams, The sulphur depletion problem. *Mon. Not. R. Astron. Soc.* **306**, 691–695 (1999).
13. M. Kama, O. Shorttle, A. S. Jermyn, C. P. Folsom, K. Furuya, E. A. Bergin, C. Walsh, L. Keller, Abundant refractory sulfur in protoplanetary disks. *Astrophys. J.* **885**, 114 (2019).

14. D. J. Hollenbach, H. A. Thronson Jr., *Interstellar Processes: Proceedings of the Symposium on Interstellar Processes, Held in Grand Teton National Park, July 1986* (Springer Science & Business Media, 2012), vol. 134.
15. E. B. Jenkins, A unified representation of gas-phase element depletions in the interstellar medium. *Astrophys. J.* **700**, 1299–1348 (2009).
16. A. Tieftrunk, G. Pineau des Forets, P. Schilke, C. M. Walmsley, SO and H_2S in low density molecular clouds. *Astron. Astrophys.* **289**, 579–596 (1994).
17. C. M. Walmsley, D. Flower, Complete depletion in prestellar cores. *Astron. Astrophys.* **418**, 1035–1043 (2004).
18. R. Friesen, J. Di Francesco, T. Bourke, P. Caselli, J. Jørgensen, J. Pineda, M. Wong, Revealing H_2D^+ depletion and compact structure in starless and protostellar cores with ALMA. *Astrophys. J.* **797**, 27 (2014).
19. L. Mattsson, Modelling dust processing and the evolution of grain sizes in the ISM using the method of moments. *Planet. Space Sci.* **133**, 107–123 (2016).
20. M. K. McClure, W. R. M. Rocha, K. M. Pontoppidan, N. Crouzet, L. E. U. Chu, E. Dartois, T. Lamberts, J. A. Noble, Y. J. Pendleton, G. Perotti, D. Qasim, M. G. Rachid, Z. L. Smith, F. Sun, T. L. Beck, A. C. A. Boogert, W. A. Brown, P. Caselli, S. B. Charnley, H. M. Cuppen, H. Dickinson, M. N. Drozdovskaya, E. Egami, J. Erkal, H. Fraser, R. T. Garrod, D. Harsono, S. Ioppolo, I. Jiménez-Serra, M. Jin, J. K. Jørgensen, L. E. Kristensen, D. C. Lis, M. R. S. McCoustra, B. A. McGuire, G. J. Melnick, K. I. Öberg, M. E. Palumbo, T. Shimonishi, J. A. Sturm, E. F. van Dishoeck, H. Linnartz, An Ice Age JWST inventory of dense molecular cloud ices. *Nat. Astron.* **7**, 431–443 (2023).
21. A. A. Boogert, P. A. Gerakines, D. C. Whittet, Observations of the icy universe. *Annu. Rev. Astron. Astrophys.* **53**, 541–581 (2015).
22. A. Boogert, W. Schutte, F. Helmich, A. Tielens, D. Wooden, Infrared observations and laboratory simulations of interstellar CH_4 and SO_2. *Astron. Astrophys.* **317**, 929–941 (1997).
23. P. M. Woods, A. Occhiogrosso, S. Viti, Z. Kaňuchová, M. E. Palumbo, S. D. Price, A new study of an old sink of sulphur in hot molecular cores: The sulphur residue. *Mon. Not. R. Astron. Soc.* **450**, 1256–1267 (2015).
24. D. P. Glavin, J. P. Dworkin, C. M. O. D. Alexander, J. C. Aponte, A. A. Baczynski, J. J. Barnes, H. A. Bechtel, E. L. Berger, A. S. Burton, P. Caselli, A. H. Chung, S. J. Clemett, G. D. Cody, G. Dominguez, J. E. Elsila, K. K. Farnsworth, D. I. Foustoukos, K. H. Freeman, Y. Furukawa, Z. Gainsforth, H. V. Graham, T. Grassi, B. M. Giuliano, V. E. Hamilton, P. Haenecour, P. R. Heck, A. E. Hofmann, C. H. House, Y. Huang, H. H. Kaplan, L. P. Keller, B. Kim, T. Koga, M. Liss, H. L. McLain, M. A. Marcus, M. Matney, T. J. McCoy, O. M. McIntosh, A. Mojarro, H. Naraoka, A. N. Nguyen, M. Nuevo, J. A. Nuth, Y. Oba, E. T. Parker, T. S. Peretyazhko, S. A. Sandford, E. Santos, P. Schmitt-Kopplin, F. Seguin, D. N. Simkus, A. Shahid, Y. Takano, K. L. Thomas-Keprta, H. Tripathi, G. Weiss, Y. Zheng, N. G. Lunning, K. Righter, H. C. Connolly, D. S. Lauretta, Abundant ammonia and nitrogen-rich soluble organic matter in samples from asteroid (101955) Bennu. *Nat. Astron.* **9**, 199–210 (2025).
25. C. Druard, V. Wakelam, Polysulphanes on interstellar grains as a possible reservoir of interstellar sulphur. *Mon. Not. R. Astron. Soc.* **426**, 354–359 (2012).
26. D. V. Mifsud, P. Herczku, R. Rácz, K. K. Rahul, S. T. S. Kovács, Z. Juhász, B. Sulik, S. Biri, R. W. McCullough, Z. Kaňuchová, S. Ioppolo, P. A. Hailey, N. J. Mason, Energetic electron irradiations of amorphous and crystalline sulphur-bearing astrochemical ices. *Front. Chem.* **10**, 1003163 (2022).
27. C. N. Shingledecker, T. Lamberts, J. C. Laas, A. Vasyunin, E. Herbst, J. Kästner, P. Caselli, Efficient production of S_8 in interstellar ices: The effects of cosmic-ray-driven radiation chemistry and nondiffusive bulk reactions. *Astrophys. J.* **888**, 52 (2020).
28. M. Garozzo, D. Fulvio, Z. Kanuchova, M. E. Palumbo, G. Strazzulla, The fate of S-bearing species after ion irradiation of interstellar icy grain mantles. *Astron. Astrophys.* **509**, A67 (2010).
29. J. C. Santos, J. Enrique-Romero, T. Lamberts, H. Linnartz, K.-J. Chuang, Formation of S-bearing complex organic molecules in interstellar clouds via ice reactions with C_2H_2, HS, and Atomic H. *ACS Earth Space Chem.* **8**, 1646–1660 (2024).
30. M. McAnally, J. Bocková, A. Herath, A. M. Turner, C. Meinert, R. I. Kaiser, Abiotic formation of alkylsulfonic acids in interstellar analog ices and implications for their detection on Ryugu. *Nat. Commun.* **15**, 4409 (2024).
31. B. Meyer, Solid allotropes of sulfur. *Chem. Rev.* **64**, 429–451 (1964).
32. P. Ferrari, G. Berden, B. Redlich, L. B. F. M. Waters, J. M. Bakker, Laboratory infrared spectra and fragmentation chemistry of sulfur allotropes. *Nat. Commun.* **15**, 5928 (2024).
33. W. Hagen, A. Tielens, J. Greenberg, The infrared spectra of amorphous solid water and ice I_c between 10 and 140 K. *Chem. Phys.* **56**, 367–379 (1981).
34. K. Fathe, J. S. Holt, S. P. Oxley, C. J. Pursell, Infrared spectroscopy of solid hydrogen sulfide and deuterium sulfide. *J. Phys. Chem. A* **110**, 10793–10798 (2006).
35. S. Maity, R. I. Kaiser, Electron irradiation of carbon disulfide-oxygen ices: Toward the formation of sulfur-bearing molecules in interstellar ices. *Astrophys. J.* **773**, 184 (2013).
36. H. Wieser, P. Krueger, E. Muller, J. Hyne, Vibrational spectra and a force field for H_2S_3 and H_2S_4. *Can. J. Chem.* **47**, 1633–1637 (2011).
37. N. Zengin, P. A. Giguère, Infrared spectrum of crystalline H_2S_2. *Can. J. Chem.* **37**, 632–634 (1959).
38. G. Socrates, *Infrared and Raman Characteristic Group Frequencies* (Wiley, ed. 3, 2004).
39. A. M. Turner, R. I. Kaiser, Exploiting photoionization reflectron time-of-flight mass spectrometry to explore molecular mass growth processes to complex organic molecules in interstellar and solar system ice analogs. *Acc. Chem. Res.* **53**, 2791–2805 (2020).
40. M. J. Abplanalp, M. Förstel, R. I. Kaiser, Exploiting single photon vacuum ultraviolet photoionization to unravel the synthesis of complex organic molecules in interstellar ices. *Chem. Phys. Lett.* **644**, 79–98 (2016).
41. A. Herath, M. McAnally, A. M. Turner, J. Wang, J. H. Marks, R. C. Fortenberry, J. C. Garcia-Alvarez, S. Gozem, R. I. Kaiser, Missing interstellar sulfur in inventories of polysulfanes and molecular octasulfur crowns. *Nat. Commun.* **16**, 5571 (2025).
42. H.-J. Werner, P. J. Knowles, P. Celani, W. Györffy, A. Hesselmann, D. Kats, G. Knizia, A. Köhn, T. Korona, D. Kreplin, R. Lindh, Q. Ma, F. R. Manby, A. Mitrushenkov, G. Rauhut, M. Schütz, K. R. Shamasundar, T. B. Adler, R. D. Amos, S. J. Bennie, A. Bernhardsson, A. Berning, J. A. Black, P. J. Bygrave, R. Cimiraglia, D. L. Cooper, D. Coughtrie, M. J. O. Deegan, A. J. Dobbyn, K. Doll, M. Dornbach, F. Eckert, S. Erfort, E. Goll, C. Hampel, G. Hetzer, J. G. Hill, M. Hodges, T. Hrenar, G. Jansen, C. Köppl, C. Kollmar, S. J. R. Lee, Y. Liu, A. W. Lloyd, R. A. Mata, A. J. May, B. Mussard, S. J. McNicholas, W. Meyer, T. F. Miller, M. E. Mura, A. Nicklass, D. P. O'Neill, P. Palmieri, D. Peng, K. A. Peterson, K. Pflüger, R. Pitzer, I. Polyak, M. Reiher, J. O. Richardson, J. B. Robinson, B. Schröder, M. Schwilk, T. Shiozaki, M. Sibaev, H. Stoll, A. J. Stone, R. Tarroni, T. Thorsteinsson, J. Toulouse, M. Wang, M. Welborn, B. Ziegler, MOLPRO 2023.1, A package of ab initio programs.
43. H.-J. Werner, P. J. Knowles, G. Knizia, F. R. Manby, M. Schütz, Molpro: A general-purpose quantum chemistry program package. *Wiley Interdiscip. Rev. Comput. Mol. Sci.* **2**, 242–253 (2012).
44. M. J. Frisch, G. W. Trucks, H. B. Schlegel, G. E. Scuseria, M. A. Robb, J. R. Cheeseman, G. Scalmani, V. Barone, G. A. Petersson, H. Nakatsuji, X. Li, M. Caricato, A. V. Marenich, J. Bloino, B. G. Janesko, R. Gomperts, B. Mennucci, H. P. Hratchian, J. V. Ortiz, A. F. Izmaylov, J. L. Sonnenberg, D. Williams-Young, F. Ding, F. Lipparini, F. Egidi, J. Goings, B. Peng, A. Petrone, T. Henderson, D. Ranasinghe, V. G. Zakrzewski, J. Gao, N. Rega, G. Zheng, W. Liang, M. Hada, M. Ehara, K. Toyota, R. Fukuda, J. Hasegawa, M. Ishida, T. Nakajima, Y. Honda, O. Kitao, H. Nakai, T. Vreven, K. Throssell, J. A. Montgomery Jr., J. E. Peralta, F. Ogliaro, M. J. Bearpark, J. J. Heyd, E. N. Brothers, K. N. Kudin, V. N. Staroverov, T. A. Keith, R. Kobayashi, J. Normand, K. Raghavachari, A. P. Rendell, J. C. Burant, S. S. Iyengar, J. Tomasi, M. Cossi, J. M. Millam, M. Klene, C. Adamo, R. Cammi, J. W. Ochterski, R. L. Martin, K. Morokuma, O. Farkas, J. B. Foresman, D. J. Fox, Gaussian 16 Revision C.01 (Gaussian Inc., 2016).
45. J. Wang, A. M. Turner, J. H. Marks, R. C. Fortenberry, R. I. Kaiser, Formation of Paraldehyde ($C_6H_{12}O_3$) in interstellar analog ices of acetaldehyde exposed to ionizing radiation. *ChemPhysChem* **25**, e202400837 (2024).
46. J. Wang, A. M. Turner, J. H. Marks, C. Zhang, N. F. Kleimeier, A. Bergantini, S. K. Singh, R. C. Fortenberry, R. I. Kaiser, Preparation of acetylenediol (HOCCOH) and glyoxal (HCOCHO) in interstellar analog ices of carbon monoxide and water. *Astrophys. J.* **967**, 79 (2024).
47. J. Wang, J. H. Marks, R. C. Fortenberry, R. I. Kaiser, Interstellar formation of glyceric acid [$HOCH_2CH(OH)COOH$]—The simplest sugar acid. *Sci. Adv.* **10**, eadl3236 (2024).
48. G. Wagner, H. Bock, Photoelektronenspektren und Moleküleigenschaften, XXVI. Die Delokalisation von Schwefel-Elektronenpaaren in Alkylsulfiden und -disulfiden. *Ber. Dtsch. Chem. Ges.* **107**, 68–77 (1974).
49. Z. Kaňuchová, P. Boduch, A. Domaracka, M. E. Palumbo, H. Rothard, G. Strazzulla, Thermal and energetic processing of astrophysical ice analogues rich in SO_2. *Astron. Astrophys.* **604**, A68 (2017).
50. M. H. Moore, R. L. Hudson, R. W. Carlson, The radiolysis of SO_2 and H_2S in water ice: Implications for the icy jovian satellites. *Icarus* **189**, 409–423 (2007).
51. W. Zheng, D. Jewitt, R. I. Kaiser, Formation of hydrogen, oxygen, and hydrogen peroxide in electron-irradiated crystalline water ice. *Astrophys. J.* **639**, 534–548 (2006).
52. R. J. Morton, R. I. Kaiser, Kinetics of suprathermal hydrogen atom reactions with saturated hydrides in planetary and satellite atmospheres. *Planet. Space Sci.* **51**, 365–373 (2003).
53. R. I. Kaiser, K. Roessler, Theoretical and laboratory studies on the interaction of cosmic-ray particles with interstellar ices. III. suprathermal chemistry-induced formation of hydrocarbon molecules in solid methane (CH_4), ethylene (C_2H_4), and acetylene (C_2H_2). *Astrophys. J.* **503**, 959 (1998).
54. B. Ruscic, D. H. Bross, Active Thermochemical Tables (ATcT) values based on ver. 1.220 of the Thermochemical Network, Argonne National Laboratory, Lemont, Illinois, USA (2025).
55. J. Hrbek, S. Y. Li, J. A. Rodriguez, D. G. van Campen, H. H. Huang, G. Q. Xu, Synthesis of sulfur films from S_2 gas: Spectroscopic evidence for the formation of S_n species. *Chem. Phys. Lett.* **267**, 65–71 (1997).
56. S. Millefiori, A. Alparone, Ab initio study of the structure and polarizability of sulfur clusters, S_n (n = 2–12). *J. Phys. Chem. A* **105**, 9489–9497 (2001).
57. M. Kumar, J. S. Francisco, Elemental sulfur aerosol-forming mechanism. *Proc. Natl. Acad. Sci. U.S.A.* **114**, 864–869 (2017).
58. M. H. Matus, D. A. Dixon, K. A. Peterson, J. A. W. Harkless, J. S. Francisco, Coupled-cluster study of the electronic structure and energetics of tetrasulfur, S_4. *J. Chem. Phys.* **127**, 174305 (2007).

59. R. Johnson, CCCBDBD Computational Chemistry Comparison and Benchmark Database (2022); http://cccbdb.nist.gov.
60. M. Fedyaeva, S. Lepeshkin, A. R. Oganov, Stability of sulfur molecules and insights into sulfur allotropy. *Phys. Chem. Chem. Phys.* **25**, 9294–9299 (2023).
61. A. M. Turner, M. J. Abplanalp, S. Y. Chen, Y. T. Chen, A. H. H. Chang, R. I. Kaiser, A photoionization mass spectroscopic study on the formation of phosphanes in low temperature phosphine ices. *Phys. Chem. Chem. Phys.* **17**, 27281–27291 (2015).
62. Y. Y. Yarnall, R. L. Hudson, A new method for measuring infrared band strengths in H_2O ices: First results for OCS, H_2S, and SO_2. *Astrophys. J. Lett.* **931**, L4 (2022).
63. R. L. Hudson, P. A. Gerakines, Infrared spectra and interstellar sulfur: New laboratory results for H_2S and four malodorous thiol ices. *Astrophys. J.* **867**, 138 (2018).
64. M. Bouilloud, N. Fray, Y. Bénilan, H. Cottin, M.-C. Gazeau, A. Jolly, Bibliographic review and new measurements of the infrared band strengths of pure molecules at 25 K: H_2O, CO_2, CO, CH_4, NH_3, CH_3OH, HCOOH and H_2CO. *Mon. Not. R. Astron. Soc.* **451**, 2145–2160 (2015).
65. A. G. Yeghikyan, Irradiation of dust in molecular clouds. II. Doses produced by cosmic rays. *Astrophysics* **54**, 87–99 (2011).
66. D. Drouin, A. R. Couture, D. Joly, X. Tastet, V. Aimez, R. Gauvin, CASINO V2.42—A Fast and easy-to-use modeling tool for scanning electron microscopy and microanalysis users. *Scanning* **29**, 92–101 (2007).
67. R. I. Kaiser, Experimental investigation on the formation of carbon-bearing molecules in the interstellar medium via neutral– neutral reactions. *Chem. Rev.* **102**, 1309–1358 (2002).
68. J. Wang, J. H. Marks, A. M. Turner, A. A. Nikolayev, V. Azyazov, A. M. Mebel, R. I. Kaiser, Mechanistical study on the formation of hydroxyacetone (CH_3COCH_2OH), methyl acetate (CH_3COOCH_3), and 3-hydroxypropanal ($HCOCH_2CH_2OH$) along with their enol tautomers (prop-1-ene-1,2-diol ($CH_3C(OH)CHOH$), prop-2-ene-1,2-diol ($CH_2C(OH)CH_2OH$), 1-methoxyethen-1-ol ($CH_3OC(OH)CH_2$) and prop-1-ene-1,3-diol ($HOCH_2CHCHOH$)) in interstellar ice analogs. *Phys. Chem. Chem. Phys.* **25**, 936–953 (2023).
69. A. Bergantini, S. Góbi, M. J. Abplanalp, R. I. Kaiser, A mechanistical study on the formation of dimethyl ether (CH_3OCH_3) and ethanol (CH_3CH_2OH) in methanol-containing ices and implications for the chemistry of star-forming regions. *Astrophys. J.* **852**, 70 (2018).
70. M. H. Moore, Studies of proton-irradiated SO_2 at low temperatures: Implications for Io. *Icarus* **59**, 114–128 (1984).
71. R. F. Ferrante, M. H. Moore, M. M. Spiliotis, R. L. Hudson, Formation of Interstellar OCS: Radiation chemistry and IR spectra of precursor ices. *Astrophys. J.* **684**, 1210–1220 (2008).
72. M. Garozzo, D. Fulvio, O. Gomis, M. E. Palumbo, G. Strazzulla, H-implantation in SO_2 and CO_2 ices. *Planet. Space Sci.* **56**, 1300–1308 (2008).
73. A. Narten, C.-G. Venkatesh, S. Rice, Diffraction pattern and structure of amorphous solid water at 10 and 77 K. *J. Chem. Phys.* **64**, 1106–1121 (1976).
74. D. M. Hudgins, S. A. Sandford, L. J. Allamandola, A. G. G. M. Tielens, Mid- and far-infrared spectroscopy of ices: Optical constants and integrated absorbances. *Astrophys. J. Suppl. Ser.* **86**, 713 (1993).
75. B. A. Seiber, A. M. Smith, B. E. Wood, P. R. Müller, Refractive indices and densities of H_2O and CO_2 films condensed on cryogenic surfaces. *Appl. Optics* **10**, 2086–2089 (1971).

Acknowledgments

Funding: The work at the University of Hawaii was funded by US National Science Foundation (NSF) Division for Astronomy (NSF-AST 2403867). We would like to thank the W.M. Keck Foundation (R.I.K.) for financing the experimental setup. **Author contributions:** R.I.K. conceived the project and designed the experiments. M.M., C.Z., J.W., A.H., and A.M.T. performed the experiments. M.M., C.Z., and R.I.K. validated the data. M.M. and R.I.K. analyzed the data, and M.M. curated the data and prepared the visualizations. R.I.K. provided resources, acquired funding, supervised the project, and administered the project, with additional supervision from A.M.T. M.M. and R.I.K. wrote the original draft. M.M., C.Z., J.W., and R.I.K. reviewed and edited the manuscript. **Competing interests:** The authors declare that they have no competing interests. **Data, code, and materials availability:** All data and code needed to evaluate and reproduce the results in the paper are present in the paper and/or the Supplementary Materials. This study did not generate new materials.

Submitted 8 August 2025
Accepted 22 May 2026
Published 10 July 2026
10.1126/sciadv.aeb3358

ScienceAdvances

Origin of sulfur allotropes on the carbonaceous asteroid Ryugu and implications to the sulfur chemistry in the interstellar medium

Mason McAnally, Chaojiang Zhang, Jia Wang, Ashanie Herath, Andrew M. Turner, and Ralf I. Kaiser

Sci. Adv. **12** (28), eaeb3358. DOI: 10.1126/sciadv.aeb3358

Science Advances (ISSN 2375-2548) is published by the American Association for the Advancement of Science. 1200 New York Avenue NW, Washington, DC 20005. The title *Science Advances* is a registered trademark of AAAS.